

Published in final edited form as:

*J Cogn Neurosci.* 2014 January ; 26(1): . doi:10.1162/jocn\_a\_00460.

## RESTING-STATE MODULATION OF ALPHA RHYTHMS BY INTERFERENCE WITH ANGULAR GYRUS ACTIVITY

Paolo Capotosto<sup>1</sup>, Claudio Babiloni<sup>2,3</sup>, Gian Luca Romani<sup>1</sup>, and Maurizio Corbetta<sup>1,4</sup>

<sup>1</sup>Department of Neuroscience e Imaging, and ITAB, Istituto di Tecnologie Avanzate Biomediche, University "G. D'Annunzio", Chieti, Italy

<sup>2</sup>Department of Physiology and Pharmacology, University of Rome "La Sapienza", Rome, Italy

<sup>3</sup>Department of Neuroscience, IRCCS San Raffaele Pisana, Rome, Italy

<sup>4</sup>Department of Neurology, Radiology, Anatomy & Neurobiology, Washington University School of Medicine, St.Louis, USA

### Abstract

The Default-Mode Networks (DMN) is active during restful wakefulness and suppressed during goal-driven behavior. We hypothesize that inhibitory interference with spontaneous ongoing, i.e. not task-driven, activity in the Angular Gyrus (AG), one of the core regions of the DMN, will enhance the dominant idling electroencephalographic (EEG) alpha rhythms observed in the resting state. Fifteen right-handed healthy adult volunteers underwent to this study. Compared to sham stimulation, magnetic stimulation (1 Hz for 1 min) over both left and right AG, but not over frontal eye field (FEF) or intra-parietal sulcus (IPS), core regions of the dorsal attention network (DAN), enhanced the dominant alpha power density (8–10 Hz) in occipito-parietal cortex. Furthermore, right AG-rTMS enhanced intra-hemispheric alpha coherence (8–10 Hz). These results suggest that AG plays a causal role in the modulation of dominant low-frequency alpha rhythms in the resting state condition.

### Keywords

Alpha rhythms; EEG; rTMS; Resting state

### Introduction

Alpha rhythms (about 8–12 Hz), first described by Hans Berger (Berger, 1929), are the most prominent feature in the electroencephalogram (EEG) of a person in a state of quiet alert wakefulness (herein "resting state"). They have predominant occipito-parietal topography, and are thought to correlate with cortical arousal and attenuated information processing. Alpha rhythms are possibly related to cortical inhibition induced by the synchronization of thalamic and cortical granular and pyramidal neurons (Steriade et al., 1990; Pfurtscheller and Lopes da Silva, 1999; Bollimunta et al., 2011).

The resting brain, as seen through the lens of functional magnetic resonance imaging (fMRI), is characterized by low frequency (about 0.1 Hz) fluctuations of the blood oxygenation signal (BOLD) that are temporally correlated across large-scale distributed

networks resembling those activated during task performance (Biswal, 1996; Fox & Raichle, 2007; Smith et al., 2009; Deco & Corbetta, 2010). One of these networks, the default mode network (DMN), originally identified as a set of parietal and medial fronto-temporal regions consistently suppressed during goal-driven behavior (Shulman et al., 1997), was noted to have tonically increased metabolic activity (Raichle et al 2001), especially glycolytic consumption (Vaishnavi et al., 2010). While many and disparate cognitive functions, including self-referential autobiographical processing (Dastjerdi et al 2011), memory retrieval (Sestieri et al. 2010; 2011), simulation of future events (Buckner et al., 2008), and suppression of irrelevant sensory events (Lewis et al., 2009; Chaddick & Gazzaley, 2011), have been proposed for the DMN, its functional importance during quiet resting wakefulness is undisputed. Also, notably, the DMN shows a competitive relationship both at rest (Fox et al 2005) and during attention and memory tasks (Sestieri et al 2010; 2013) with the so called dorsal attention network (DAN; Corbetta & Shulman, 2002; Corbetta & Shulman, 2011), a set of frontoparietal regions involved in the selection of behaviorally relevant sensory-motor information. For instance, during visual selection tasks, the DAN is strongly recruited while the DMN is suppressed, while during retrieval of memory information the reverse occurs (Sestieri et al 2010).

The relationship between activity in the DMN and alpha band power in the awake restful state has been investigated with conflicting results by recording simultaneously EEG rhythms and fMRI BOLD signals. While one study found a positive correlation between fluctuations of the BOLD signals in the DMN at rest and alpha power fluctuations (Mantini et al., 2007), others reported either weak or no correlation (Gonçalves et al., 2006; Laufs et al., 2003; Knyazev et al., 2011; Wu et al., 2010). In contrast, more consistent and robust negative correlations have been reported between BOLD signal fluctuations in the DAN and alpha power (Sadaghiani et al., 2010; Mantini et al., 2007; Laufs et al., 2003), and BOLD signal fluctuations in the DMN and beta power (Laufs et al. PNAS 2003; Mantini et al. PNAS 2007). This brief review indicates that the relationship between BOLD signals fluctuations in specific cortical networks and EEG rhythms is complex.

Correlations between fMRI BOLD and EEG signals are quite interesting, but provide only indirect evidence for a causal relationship between these two sets of signals. More direct evidence about the generation or modulation of cortical rhythms can be obtained by examining the effects of excitatory or inhibitory repetitive trans-cranial magnetic stimulation (rTMS) to a given cortical region onto the ongoing EEG rhythms.

We have recently used this method to study the causal role of Dorsal Attention regions, IPS and FEF, in the control of anticipatory (pre-target) occipito-parietal alpha de-synchronization, a putative correlate of top-down attention control (Capotosto et al., 2009; 2012a). Interference with IPS and FEF preparatory activity following a spatial cue induced an abnormal enhancement of alpha rhythms in the occipital-parietal region contra-lateral to the expected visual stimuli, consistent with a disruption of top-down modulation (Capotosto et al., 2009; 2012a).

Here, we test the role of a core region of the DMN, the Angular Gyrus (AG), in the modulation of alpha rhythms under the assumption that this region is spontaneously active during rest (Raichle, 2001) and that mediates ongoing internally directed cognitive processes (Sestieri et al 2010). Accordingly, suppression of AG by rTMS at rest should produce, as in the case of DAN regions during attention, an abnormal increase in alpha power in posterior cortical regions where alpha rhythms are typically dominant in the resting state condition. Furthermore, the propagation of the inhibitory enhancement of alpha rhythms are expected to be preponderant in the hemisphere ipsilateral to TMS interference, due to the well known more efficient functional connectivity within any hemisphere. To ascertain the location- and

frequency-specificity of these effects, and in relation to the inverse relationship between alpha and beta rhythms, and BOLD fluctuations, respectively, in the DAN (Sadaghiani et al., 2010; Mantini et al., 2007; Laufs et al., 2003), and DMN (Laufs et al. PNAS 2003; Mantini et al. PNAS 2007), core nodes of the DAN (IPS, FEF) were also tested, and the frequency analysis was extended to both alpha and beta bands.

## Materials and Methods

### Subjects

Fifteen right-handed (Edinburgh Inventory) healthy adult volunteers (age range: 21–27 yrs old; 6 females) with no previous psychiatric or neurological history participated to the experiment. Their vision was normal or corrected-to-normal. All experiments were conducted with the understanding and written consent of each participant according to the Code of Ethics of the World Medical Association, and the standards established by the University of Chieti Institutional Review Board and Ethics Committee.

### Experimental task

All measurements were carried out at the Institute of Technology and Advanced Bioimaging (ITAB) by the first author (P.C.). Subjects were seated in a comfortable reclining armchair. They maintained fixation on a small white cross stimulus (subtending  $0.7^\circ$  of visual angle) displayed on a black background in the center of a computer screen positioned at a distance of 80 centimeters.

### Procedures for rTMS and identification of target scalp regions

Repetitive TMS was used to interfere with neural activity. The stimulation was delivered through a focal, figure eight coil (outer diameter of each wing 7 cm) connected with a standard Mag-Stim Rapid 2 stimulator (maximum output 2.2 Tesla). A mechanical arm maintained the handle of the coil angled at about  $45^\circ$  away from the midline. The exact position was adjusted based on the results of the on-line neuronavigation such that the center of the coil wing was oriented perpendicularly to the point to be stimulated with the maximum power. The center of the coil wings was positioned at a position on the scalp corresponding to the each cortical region of interest. Individual resting excitability threshold for right motor cortex stimulation was preliminarily determined by following standardized procedures (Rossini et al., 1994). The rTMS train was delivered based on the following parameters: 1-minute duration, 1-Hz frequency, and intensity set at 100% of the individual motor threshold. These parameters are consistent with published safety guidelines for TMS stimulation (Anderson et al., 2006; Machii et al., 2006; Wassermann, 1998; Rossi et al., 2009). Of note, 1-Hz rTMS for 1 minute is thought to inhibit the target cortical area for 1 or 2 minutes post-stimulation (Pascual-Leone et al., 1998).

The experimental design included seven conditions, applied in different blocks, and randomized across subjects. Each subject performed all the conditions. Two consecutive TMS sessions were separated by an interval of about 5 min. In the ‘Sham’ condition the stimulation was delivered at the scalp vertex with the position of the coil reversed with respect to the scalp surface, such that the magnetic flux was dispersed in the air. In the six active conditions the center of the coil wings was positioned at a position on the scalp corresponding to different cortical regions obtained from a meta-analysis of spatial attention studies (He et al., 2007; Fox et al., 2005). Four of these regions corresponded to core regions of the DAN: i) right pIPS ( $x,y,z: 23,-65,48$ ), left pIPS ( $x,y,z:-25,-63, 47$ ), right FEF ( $x,y,z: 32,-9,48$ ), left FEF ( $x,y,z:26,-9, 48$ ). The two other regions are hubs of the DMN: right AG ( $x,y,z: 53,-67,46$ ), left AG ( $x,y,z:-47,-67, 36$ ). The positioning of the TMS coil onto the subjects’ scalp was based on a procedure developed as part of the SoftTaxic software that

allows to reconstruct an individualized head model based on a set of digitized skull landmarks (nasion, inion, and two pre-auricular points) and on about 40 scalp points entered with a Fastrak Polhemus digitizer system (Polhemus). Such model is then warped to a standard mean MRI-based head template (152 subjects – Statistical Parametric Mapping SPM-tool version 2) through affine linear transformation. The present procedure has been successful in previous rTMS studies (Babiloni et al. 2006; Harris et al., 2008; Capotosto et al. 2009, 2012a, 2012b; Urgesi et al., 2004, 2007; Candidi et al., 2011; Sestieri et al. 2013). Of note, while in our pilot studies we observed that rTMS over a ventral region (i.e. right TPJ, mean coordinates X=52, Z=-49, and Y=17) caused scalp and face muscular twitches and subjects' discomfort, in the present study none of the subjects declared any kind of discomfort (i.e. pain) during each experimental conditions.

### Electroencephalography recordings

EEG data were recorded (BrainAmp; bandpass, 0.05–100Hz, sampling rate, 256 Hz) from 27 EEG electrodes placed according to an augmented 10–20 system, and mounted on an elastic cap resistant to magnetic pulses. Electrode impedance was below 5 K. The artifact of rTMS on the EEG activity lasted about 10 ms and did not generate any alteration in the power spectrum. Two electro-oculographic channels were used to monitor eye movement and blinking. The acquisition time for all conditions was set from -1.5 to +0 min before rTMS train onset, and from +1 to +3 min after the rTMS train onset. EEG data were segmented off-line in windows of 2 sec. The intensive experimental design (6 active TMS condition and 1 sham) imposed this limitation in the time extension of the rTMS and of the post-stimulation periods, to minimize fatigue and drops of vigilance. The EEG single trials contaminated by eye movement, blinking, or involuntary motor acts (e.g. mouth, head, trunk or arm movements) were rejected off-line. To remove the effects of the electric reference, EEG single trials were re-referenced by the common average reference. The common average procedure includes the averaging of amplitude values at all electrodes and the subtraction of the mean value from the amplitude values at each single electrode.

The EEG data analysis was performed in the following periods of interest: (i) “pre-TMS” (1.5 minutes before rTMS train and offline segmented in windows of 2 sec), (ii) “post-TMS 1” (the first minute after rTMS train and offline segmented in windows of 2 sec), and (iii) “post-TMS 2” (the second minute after rTMS train and offline segmented in windows of 2 sec). The mean number of trials per EEG segments of 2 s was 42 ( $\pm 3$ ) for the pre-TMS period and 86 ( $\pm 4$ ) for the post-TMS period. Of note, EEG datasets of one subject were excluded since the profile of EEG power density spectra was clearly abnormal/artifactual in several TMS conditions.

### Analysis of EEG power

We measured the effect of rTMS at different cortical loci on the power of alpha and beta rhythms in parieto-occipital cortex. The EEG power, in a matrix of scalp electrodes, reflects the spatial and temporal summation of synchronous activity of cortical neurons whose synaptic currents are associated to changes of the voltage at those electrodes. For the EEG spectral analysis, two sub-bands of alpha rhythms were used, namely low- and high-frequency alpha. These sub-bands were determined in accordance to a standard procedure based on the peak of individual alpha frequency (IAF; Klimesch et al., 1998). With respect to the IAF, these frequency bands were defined as follows: (i) low-alpha, IAF - 2 Hz to IAF, and (ii) high-alpha, IAF to IAF + 2 Hz. Moreover, with respect to the individual beta frequency (IBF) peak, for the EEG spectral analysis, we also used two sub-bands of beta rhythms, namely low- and high-frequency beta, defined as follows: (i) low-beta, IBF - 2 Hz to IBF, and (ii) high-beta, IBF to IBF + 2 Hz. Of note, mean IAF peak across subjects was 10.1 Hz ( $\pm 0.2$  SE), and mean IBF peak across subjects was 18.9 Hz ( $\pm 0.5$  SE). No

statistically significant difference was observed across the rTMS conditions ( $p > 0.05$ ) for both alpha and beta peaks.

### Estimation of the functional connectivity: between-electrode coherence analysis

The effect of rTMS at different cortical loci was also tested on the coherence of alpha and beta rhythms at electrode pairs, as an estimation of the functional coupling of EEG rhythms at different cortical sites. Spectral coherence is a normalized measure of the coupling between two (EEG) signals at any given frequency (Rappelsberger and Petsche, 1988; Pfurtscheller and Andrew, 1999). The coherence values were calculated for each frequency bin by the following equation:

$$\text{Coh}_{xy}(\ddot{e}) = |\text{R}_{xy}(\ddot{e})|^2 = |\text{f}_{xy}(\ddot{e})|^2 / [\text{f}_{xx}(\ddot{e})\text{f}_{yy}(\ddot{e})]$$

The above equation is the extension of the Pearson's correlation coefficient to complex number pairs. In this equation,  $f$  denotes the spectral estimate of two EEG signals  $x$  and  $y$  for a given frequency bin ( $\ddot{e}$ ). The numerator contains the cross-spectrum for  $x$  and  $y$  ( $\text{f}_{xy}$ ), while the denominator contains the respective autospectra for  $x$  ( $\text{f}_{xx}$ ) and  $y$  ( $\text{f}_{yy}$ ). For each frequency bin ( $\ddot{e}$ ), the coherence value ( $\text{Coh}_{xy}$ ) is obtained by squaring the magnitude of the complex correlation coefficient  $R$ . This procedure returns a real number between 0 (no coherence) and 1 (max coherence).

For the evaluation of the inter-hemispheric spectral coherence, the electrode pairs were F3–F4 (frontal areas), C3–C4 (central areas), P7–P8 (parietal areas), O1–O2 (occipital areas), and T7–T8 (temporal areas). For the evaluation of the intra-hemispheric spectral coherence, the electrode pairs were F3–P3 (fronto-parietal), F3–O1 (fronto-occipital), and F3–T3 (fronto-temporal) for the left hemisphere and F4–P4 (fronto-parietal), F4–O2 (fronto-occipital), and F4–T4 (fronto-temporal) for the right hemisphere. The coherence of the EEG data was computed in the baseline pre-TMS period and in the post-stimulus period (namely, Post-TMS 1 and Post-TMS 2) for the mentioned seven conditions (i.e. Sham, Left-AG, Right-AG, Left-IPS, Right-IPS, Left-FEF, and Right-FEF).

Of note, EEG coherence is not mathematically independent of power of the EEG signal at electrode sites, as they result from the computation of Fast Fourier Transform. However, the two indexes do not provide redundant information. For example, the alpha power in a matrix of scalp electrodes reflects the spatial and temporal summation of synchronous activity of cortical neurons at about 10 Hz whose synaptic currents are associated to changes of the voltage at those electrodes. Alpha coherence among pairs of those electrodes is related to the linear interdependence of the alpha rhythms among specific pairs of electrodes. More analytically, consider the case in which the electrodes A, B, and C of the matrix have the same amount of alpha power. The coherence in alpha band between the electrode A and the two electrodes B and C can be markedly different as a function of relative distance and underlying structural brain connectivity. Keeping in mind these considerations, one cannot predict the amplitude of the EEG coherence between electrode pairs only on the basis of EEG power at the corresponding electrodes.

### Statistical analysis

Statistical comparisons were performed by ANOVAs for repeated measures. We used a Mauchly's test to evaluate the sphericity assumption of the ANOVA, a Greenhouse-Geisser procedure for the correction of the degrees of freedom based, and Duncan tests for post-hoc comparisons ( $p < 0.05$ ).

The ANOVAs aimed at unveiling the most effective sites of rTMS stimulation and the topographical localization of the most important effects on alpha rhythms. Due to the relatively small population size, separate simple ANOVA designs were used for alpha sub-bands (low- and high-frequency) and TMS sites. For the ANOVAs using EEG power density as a dependent variable, Time (Pre-TMS, Post-TMS 1, Post-TMS 2) and Electrode (F3, F4, C3, C4, T7, T8, P7,P8, O1, O2) served as within-subject factors. For the ANOVAs using spectral coherence as a dependent variable, Topology (Inter-hemispheric, Right Intra-hemispheric, and Left Intra-hemispheric) and Time (Pre-TMS, Post-TMS 1, Post-TMS 2) served as within-subject factors. The inter-hemispheric coherence was defined as the mean of the coherence values across frontal (F3-F4), central (C3-C4), parietal (P7-P8), temporal (T7-T8) and occipital (O1-O2) electrode pairs. For the left intra-hemispheric coherence, the coherence values were averaged across fronto-parietal (F3-P3), fronto-occipital (F3-O1), and fronto-temporal (F3-T3). For the right intra-hemispheric coherence, the coherence values were averaged across fronto-parietal (F4-P4), fronto-occipital (F4-O2), and fronto-temporal (F4-T4).

Considering the amount of factors (i.e. Time and Electrode), relative levels and population size, an ANOVA design including all TMS sites would have been inappropriate as a main statistical analysis. Nevertheless, we performed an exploratory analysis to directly compare the effects of the rTMS over DMN and DAN networks on posterior resting state EEG rhythms. Specifically, we computed two exploratory ANOVAs, one using EEG power density as a dependent variable and the other using spectral coherence. In the first exploratory ANOVA, we averaged the alpha power values across selected parieto-occipital electrodes (i.e. P7, P8, O1, O2) and the rTMS conditions relative to a single cortical network (i.e. DMN, DAN). For the DMN, the alpha power density for the left and right AG was averaged. For the DAN, the alpha power density for bilateral IPS and FEF was averaged. On the whole, the first exploratory ANOVA included Network (DMN and DAN; independent variable) and Time (Pre-TMS, Post-TMS 1, Post-TMS 2) as within-subject factors. In the second exploratory ANOVA, we averaged the alpha coherence across all electrode pairs and the rTMS conditions relative to a single cortical network as well. For the DMN, the alpha coherence for the left and right AG was averaged. For the DAN, the alpha coherence for bilateral IPS and FEF was averaged. On the whole, the second exploratory ANOVA included Network (DMN and DAN; independent variable), Hemisphere (ipsilateral or contralateral to the stimulation) and Time (Pre-TMS, Post-TMS 1, Post-TMS 2) as within-subject factors.

To test the frequency-specific effect of rTMS on the alpha rhythms, we performed an analogue analysis on beta power and coherence. Separate ANOVAs were designed for beta sub-bands (low- and high-frequency) and TMS sites. For the ANOVAs using EEG beta band power density as a dependent variable, Time (Pre-TMS, Post-TMS 1, Post-TMS 2) and Electrode (F3, F4, C3, C4, T7, T8, P7,P8, O1, O2) served as within-subject factors. For the ANOVAs using spectral beta coherence as a dependent variable, Topology (Inter-hemispheric, Right Intra-hemispheric, and Left Intra-hemispheric) and Time (Pre-TMS, Post-TMS 1, Post-TMS 2) served as within-subject factors. Furthermore, to directly compare the effect of the rTMS over DMN and DAN, we used ANOVAs for the beta band (averaging low and high beta) in line with those used for the analysis of the alpha band.

To rule out effects of rTMS on baseline alpha power (pre-TMS period), two ANOVAs used Condition (Sham, Right-AG, Left-AG, Right-IPS, Left-IPS, Right-FEF, Left-FEF) and Electrode (F3, F4, C3, C4, T7, T8, P7,P8, O1, O2) as within subject factors. The two ANOVAs were focused on low- and high-frequency alpha sub-bands, respectively.

## Results

### Alpha power density

Figure 1a shows the topographic maps of low- and high-frequency alpha power density in the Sham condition during the three periods of interest (Pre-TMS, Post-TMS 1, Post-TMS 2). Figure 1b shows the mean alpha power density, separately for low and high alpha, in different electrodes and periods of interest. Resting-state alpha power density was higher in amplitude over the parieto-occipital regions in all periods of interest, and Sham stimulation did not produce any significant modulation ( $p>0.05$ ). This analysis rules out any consistent effect of Sham or other experimental procedures on the resting state alpha rhythms.

Figure 2 shows the low-frequency alpha power density for Right-AG, Left-AG, Right-IPS, Left-IPS, Right-FEF, and Left-FEF conditions during the three periods of interest (Pre-TMS, Post-TMS 1, Post-TMS 2) respectively. In all conditions the resting-state alpha power density was higher in amplitude at bilateral parietal and occipital electrodes. At these electrodes, right AG stimulation induced a progressive increase of alpha power in the first (Post-TMS 1) and second minute (Post-TMS 2) after stimulation. This impression was confirmed by a statistical analysis showing a significant interaction between Time and Electrode factors for right AG ( $F(18,234)=1.85$ ;  $p<0.02$ ). Post-hoc tests indicated an increment of low-frequency alpha power density at occipital-parietal electrodes during the post-TMS 1 (P7  $p<0.05$ ; O1  $p<0.03$ ) and post-TMS 2 periods (P7  $p<0.0001$ ; P8  $p<0.05$ ; O1  $p<0.0001$ ; O2  $p<0.01$ ) (Figure 2). A similar effect was also observed for left AG ( $F(18,234)=1.64$ ;  $p<0.05$ ) stimulation condition. Post-hoc tests indicated an increment of low-frequency alpha power density at occipital-parietal electrodes during the post-TMS 1 (P7  $p<0.01$ ; P8  $p<0.0001$ ; O1  $p<0.01$ ; O2  $p<0.02$ ) and post-TMS 2 periods (P7  $p<0.02$ ; O1  $p<0.04$ ; O2  $p<0.01$ ; Figure 2). These increments were not observed at the high-frequency alpha sub-band. These findings were found to be specific for the stimulation of DMN. Statistical analysis showed no significant effect of rTMS over Right-IPS, Left-IPS, Right-FEF, and Left-FEF (i.e. DAN) on alpha power density ( $p>0.05$ ).

Finally, a control analysis for each condition was performed to test the main effect Time on the low-frequency alpha power density. With respect to the ANOVAs of the main analysis, the same within-subject factors were used. As a difference, only the parieto-occipital electrodes of interest (i.e. P7, P8, O1, O2) were used. We observed that only the inhibitory rTMS over right AG produced a main effect Time ( $F(2,26)=3.62$ ;  $p<0.04$ ), while the rTMS over left AG produced a marginal statistical effect ( $F(2,26)=3.10$ ;  $p=0.06$ ), thus globally confirming the results of the main analysis.

### Alpha spectral coherence

In line with the results of alpha power density, Sham stimulation produced no statistically significant effect on alpha coherence ( $p>0.05$ ).

Figure 3 shows the low-frequency mean alpha coherence for Right-AG, Left-AG, Right-IPS, Left-IPS, Right-FEF, and Left-FEF conditions during the three periods of interest (Pre-TMS, Post-TMS 1, Post-TMS 2), respectively. The alpha coherence values were averaged across electrode pairs to index inter-hemispheric, left intra-hemispheric, and right intra-hemispheric coherence (see Methods). In all conditions mean coherence was higher in inter- than intra-hemispherical indexes regardless of rTMS conditions ( $p<0.001$ ). For these indexes, right AG stimulation induced a progressive increase of alpha coherence along Post-TMS 1 and Post-TMS 2 periods. Again, statistical analysis showed that the only remarkable effect of the rTMS on alpha coherence was observed for the magnetic stimulation of DMN but not DAN. Only for the stimulation of right AG, there were statistically significant effects. Specifically, there was an interaction between Topology and Time factors ( $F(4,52)=3.05$ ;  $p<0.03$ ),

indicating the increase of the right intra-hemispheric low-frequency alpha coherence during post-TMS 1 and post-TMS 2 ( $p < 0.0001$ ). A mirror effect of left AG stimulation on the left intra-hemispheric low-frequency alpha coherence did not reach the statistical significance ( $p > 0.05$ ). These increments were not observed in the high-frequency alpha sub-band.

Finally, control ANOVAs considering separately each Topology of the coherence (i.e. right hemisphere, left hemisphere) were computed to the main effect Time. The results of the main analysis were confirmed. In particular, an ANOVA using right intra-hemispheric coherence (i.e. ipsilateral to the stimulation) as a dependent variable and Time (Pre-TMS, Post-TMS 1, Post-TMS 2) as within-subject factor showed a main effect Time for the rTMS over right AG ( $F(2,26) = 3.57$ ;  $p = 0.04$ ). Post-hoc test indicated an increase of the right intra-hemispheric low-frequency alpha coherence during post-TMS ( $p < 0.02$ ). The counterpart using left intra-hemispheric coherence (i.e. ipsilateral to the stimulation) as a dependent variable only provided statistically marginal results ( $F(2,26) = 2.69$ ;  $p = 0.08$ ).

### DMN vs. DAN

To compare the effect of rTMS over the two networks on the low-frequency alpha power density, we performed an ANOVA with Network (DMN, DAN; after averaging over nodes), Hemisphere (Left, Right), and Time (Pre-TMS, Post-TMS 1, Post-TMS 2). Figure 4a shows the low-frequency mean alpha power density for DMN (after averaging Right-AG and Left-AG) and DAN (after averaging Right-IPS, Left-IPS, Right-FEF, and Left-FEF) during the three periods of interest (Pre-TMS, Post-TMS 1, Post-TMS 2), respectively. Although the interaction between Networks and Time did not reach the statistical significance ( $p = 0.085$ ), rTMS over DMN induced a progressive increase of the alpha power in the first (Post-TMS 1) and in the second minute (Post-TMS 2) after magnetic stimulation. This effect was not observed for rTMS over DAN.

Figure 4b shows the low-frequency mean alpha coherence for DMN (after averaging Right-AG and Left-AG) and DAN (after averaging Right-IPS, Left-IPS, Right-FEF, and Left-FEF) during the three periods of interest (Pre-TMS, Post-TMS 1, Post-TMS 2), respectively, separated by Hemisphere (ipsilateral or contralateral to the stimulation). Statistical analysis showed that the only significant effect of the rTMS on alpha coherence was observed for the magnetic stimulation of DMN (AG) but not DAN. Specifically, there was an interaction between Network and Time ( $F(2,26) = 3.21$ ;  $p = 0.05$ ), and an interaction between Network, Hemisphere, and Time factors ( $F(2,26) = 4.58$ ;  $p = 0.02$ ), indicating that DMN (AG) magnetic stimulation induced a progressive increase of the ipsilateral intra-hemispheric low-frequency alpha coherence during post-TMS 1 and post-TMS 2 ( $p < 0.0001$ ). A similar trend was also observed stimulating DMN for the contralateral intra-hemispheric low-frequency alpha coherence. Of note, no statistically significant results were observed for both power and coherence in the high frequency alpha sub-band.

### Beta power density and spectral coherence

For both low- and high-beta power and coherence, no statistically significant interaction was observed for the interference of rTMS ( $p > 0.05$ ). The same lack of statistical effects ( $p > 0.05$ ) was observed when DMN and DAN were compared in the beta band (Fig. 5). There was only a trend similar to that observed in the alpha band, especially for the EEG coherence ipsilateral to the stimulation site (e.g. right AG). These results suggest a more strict causal relationship between AG and the modulation of alpha compared to beta rhythms in the resting state condition.



## Control analyses

Control statistical analysis showed no significant difference of the alpha power density in the pre-TMS period (baseline) among Sham, Right-AG, Left-AG, Right-IPS, Left-IPS, Right-FEF, and Left-FEF conditions ( $p>0.05$ ). This was true for both low- and high-frequency alpha sub-bands. These findings confirmed that the main results were not due to different baseline alpha power density among the conditions of magnetic stimulation.

## Discussion

There exists a classic relationship between a state of resting wakefulness and the presence of a dominant alpha rhythm on the EEG (Berger, 1929). More recently, the resting state has been associated with tonic metabolic and neural activity in the DMN, a distributed fronto-temporal-parietal cortical network active at rest (Raichle et al. 2001; Vaishnavi et al., 2010). We tested the hypothesis that AG plays a causal role in the modulation of resting state alpha rhythms in the posterior cortical regions, under the assumption that DMN regions are active in the resting state possibly in support of internally directed cognition (Sestieri et al. 2010). In agreement with this hypothesis, we found that inhibitory (1 Hz) rTMS stimulation of the AG for one minute enhanced alpha power in both hemispheres in the post-stimulus period (i.e. 1st and 2nd minute post-stimulation). This modulation was stronger for right AG stimulation, which also produced increased alpha spectral coherence ipsilaterally in the right hemisphere. Critically these effects were specific for AG. Sham stimulation and magnetic stimulation of two nodes of the DAN (i.e. FEF and IPS on either hemisphere) did not produce any significant modulation of alpha power or coherence. In addition, the modulation was also not only location-specific, but also frequency-specific to the low frequency alpha rhythms (8–10 Hz), and did not extend to the high frequency alpha rhythms (10–12 Hz). This is consistent with a model in which different frequencies of alpha rhythms reflect different functional modes of thalamo-cortical and cortico-cortical loops that facilitate/inhibit the transmission and retrieval of sensorimotor and cognitive information (Pfurtscheller and Lopes da Silva 1999). Specifically, it has been proposed that low-frequency alpha rhythms would diffusely regulate global brain arousal and alertness, whereas high-frequency alpha rhythms would reflect task-related oscillations of selective neural systems involved in the elaboration of task-specific information (Klimesch et al., 1998). The frequency-specific effect of rTMS over DMN was further supported by a lack of modulation in the beta band.

Overall these findings albeit exploratory strongly suggest a direct ‘causal’ link between activity in the AG at rest and modulation/generation of alpha rhythms. Several open questions remain.

One question concerns the physiological mechanisms underlying this modulation. Repeated 1-Hz stimulation of neocortex by rTMS is thought to cause a (partial) suppression of excitatory synaptic transmission (Thickbroom, 2007; Ridding & Ziemann, 2010), and induces long-term specific changes in the expression of c-Fos (Aydin-Abidin et al. 2008; Funke & Benali 2010) and GABA-synthesizing enzymes (Trippe et al. 2009; Funke & Benali 2010). A reduction in calcium-binding protein calbindin in inhibitory interneurons modulating the activity of pyramidal cells has been also reported (Funke and Benali, 2010). Therefore, 1-Hz TMS stimulation is expected to tonically suppress neuronal activity. Based on our study the effect extended for two minutes following one minute stimulation in AG. We selected our stimulation and post-stimulation periods based on an important study that showed that low-frequency (i.e. 1 Hz) rTMS over motor cortex induces an inhibitory enhancement of the alpha rhythms for a period corresponding to that of the magnetic stimulation (Brignani et al., 2008). Interestingly, in our study modulation of alpha power extended significantly into the second minute post-stimulation suggesting that AG

suppression is more prolonged than motor cortex. This may be due to the more central position of AG in the neuroanatomical matrix of connections and networks (see below) (Hagmann et al., 2008; Buckner et al., 2009). Follow up studies will need to trace the time-course of this tonic inhibition, thus also allowing a full recovery of the effects to baseline and the reconstruction of the timing of the effect peak and plateau. Furthermore, they may include an active control TMS condition targeting scalp vertex (a region here used as Sham) as a site where TMS elicits no muscle activation (Mutanen et al., 2013). The relative results would refine the understanding of the neural basis of the present results, although we did not observe any remarkable discomfort or muscle interference stimulating over regions of DAN and DMN.

Since cortical alpha rhythms are presumed to be generated by the oscillatory activity of granular and pyramidal neurons, mainly based on the input signals delivered by relay-mode and high-threshold bursting thalamo-cortical neurons (Lorincz et al., 2009; Bollimunta et al., 2011), our results suggest that suppression of AG activity modulated either cortical parieto-occipital regions where alpha rhythms localize or their thalamo-cortical inputs (Srinivasan et al., 2006).

The modulation of alpha rhythms did not remain local, but spread, especially for right AG stimulation, ipsilaterally across other cortical sites as demonstrated by a diffuse increased intra-hemispheric coherence as compared to other cortical sites (e.g. IPS and FEF). One possible explanation for the increase in intra-hemispheric coherence is the previously noted central position of AG in the structural/functional neuroanatomical matrix of the brain (Hagmann et al., 2008; Buckner et al., 2009). It is also consistent with recent magnetoencephalographic (MEG) evidence from our group showing that the DMN is a hub of inter-network cortical interactions in the resting state especially in the alpha and beta frequency bands (de Pasquale et al., 2012).

Another important question is the relationship of our results to the extant fMRI-EEG literature. The enhancement of alpha power after AG suppression is apparently in contradiction with some studies that find a positive relationship between alpha power and BOLD signal fluctuations in the DMN at rest (e.g. Mantini et al., 2007; but see: Gonçalves et al., 2006; Laufs et al., 2003; Knyazev et al., 2011; Wu et al., 2010). Similarly, lack of modulation after suppression of DAN nodes (IPS, FEF) apparently contradicts the negative relationship between alpha power and BOLD signal fluctuations in the DAN at rest (Sadaghiani et al., 2010; Mantini et al., 2007; Laufs et al., 2003). However, one should consider the different time-scale over which these effects are measured with different methods. In our study, effects were transient lasting for only a couple of minutes after stimulation. In contrast EEG/fMRI correlations are recorded and maintain significance over tens of minutes. Another major difference is the spatial resolution that is more precise with fMRI than EEG. For instance it would be important to separate the direct effect of rTMS suppression on AG activity vs. the indirect modulation on other regions. To this effect, it is important to underscore that scalp alpha rhythms reflect the summation of neural currents generated by different processes and cortical regions, including regions that are active hence de-synchronized and regions that are relatively suppressed hence more synchronized. This summation at the scalp level might confound the interpretation of the “correlation” in EEG-fMRI studies.

A third issue concerns the functional significance of the alpha power/coherence enhancement after AG stimulation. Our interpretation assumes that posterior parieto-occipital alpha rhythm underlies a state of ‘idling’ or partial inactivity of cortical information processing in relation to external stimuli. Task-related recruitment of cortex de-synchronizes low/intermediate EEG frequencies including alpha and beta, but synchronizes

higher EEG frequencies including gamma (Crone et al., 2006; Miller et al., 2009; Canolty et al., 2007; Siegel et al., 2009; Fries et al 2011; Freunberger et al., 2007). The degree of alpha synchronization in occipital-parietal sensory regions is putatively controlled during perceptual tasks by higher-order cortical regions involved in top-down control (Corbetta & Shulman, 2002; Fries, 2005). As a result, occipito-parietal alpha power is high in a state of idleness (rest), decreases during visual (attention) tasks (e.g. Worden et al. 2000; Thut et al. 2006), and paradoxically increases when regions of the DAN presumably controlling the allocation of attention are (partially) inactivated by inhibitory rTMS (Capotosto et al., 2009, 2012a).

By analogy, if the AG is involved in internally directed cognition such as memory retrieval (Sestieri et al. 2010, 2012) or simulation of the future (Buckner, 2010), and these processes are spontaneously active at rest as suggested by metabolic studies (Raichle et al 2001; Visnashari et al 2010), then inactivation of AG is expected to cause a local inhibitory increase in alpha power as well as a propagation of such perturbation across the cerebral cortex, especially in the occipito-parietal regions where alpha rhythms show maximum power. This view assumes that AG plays a role of neural “hub” and propagates the synchronization/desynchronization of low-frequency alpha rhythms across the cerebral cortex. In this framework, alpha power would index the magnitude of cortical inhibition in task relevant representations, both related to external cognition (e.g. DAN) or internal cognition (e.g. DMN).

A final point of discussion is the right lateralization of the modulation of intra-hemispheric coherence, which was stronger for right over left AG. Alpha rhythms are traditionally associated with attention and arousal (Babiloni et al., 2003; Haegens et al., 2012). Arousal deficits are classically associated with right hemisphere lesions (Corbetta & Shulman 2011) including regions of the inferior parietal lobule (supramarginal, SMG, and AG). While AG is part of the DMN, the SMG along with the temporoparietal junction is part of the so called ventral attention network that is right hemisphere lateralized (Shulman et al 2010; Corbetta & Shulman, 2011; Liu et al., 2009). These regions have been also implicated in arousal and vigilance (Corbetta & Shulman, 2011). In the present study, the right lateralization on alpha coherence may partly reflect a certain suppression of adjacent cortex in SMG.

## Conclusions

Inhibitory magnetic stimulation over bilateral AG, one of the core DMN nodes, but not FEF or IPS, core DAN nodes, enhanced resting state, low-frequency alpha power in bilateral occipito-parietal cortex, as well as intra-hemispheric alpha coherence (right AG). These results suggest that AG plays a causal role in the modulation and propagation of the resting state dominant alpha rhythms to the posterior parietal regions.

## Acknowledgments

The research leading to these results has received funding from the European Community's Seventh Framework Programme (FP7/2007–2013), Grant Agreement ‘BrainSynch’ n° HEALTH-F2-2008-200728”. M.C was supported by the National Institute of Mental Health, grants R01 1R01MH096482 and HD061117-05A2 P.C. was supported by a post-doctoral contract from the “G. D’Annunzio University” Foundation, Chieti, Italy. C.B was supported by the Italian Ministry of Health, project GR-2008-1143091.

## REFERENCES

- Anderson B, Mishory A, Nahas Z, Borckardt JJ, Yamanaka K, Rastogi K, George MS. Tolerability and safety of high daily doses of repetitive transcranial magnetic stimulation in healthy young men. *J Ect.* 2006; 22:49–53. [PubMed: 16633208]

- Aydin-Abidin S, Trippe J, Funke K, Eysel UT, Benali A. High- and low-frequency repetitive transcranial magnetic stimulation differentially activates c-Fos and zif268 protein expression in the rat brain. *Exp Brain Res*. 2008 Jun; 188(2):249–261. Epub 2008 Apr 2. [PubMed: 18385988]
- Babiloni C, Vecchio F, Miriello M, Romani GL, Rossini PM. Visuo-spatial consciousness and parieto-occipital areas: a high-resolution EEG study. *Cereb Cortex*. 2006; 16(1):37–46. [PubMed: 15800023]
- Babiloni C, Cassetta E, Binetti G, Tombini M, Del Percio C, Ferreri F, Ferri R, Frisoni G, Lanuzza B, Nobili F, Parisi L, Rodriguez G, Frigerio L, Gurzi M, Prestia A, Vernieri F, Eusebi F, Rossini PM. Resting EEG sources correlate with attentional span in mild cognitive impairment and Alzheimer's disease. *Eur J Neurosci*. 2007 Jun; 25(12):3742–3757. [PubMed: 17610594]
- Babiloni C, Brancucci A, Babiloni F, Capotosto P, Carducci F, Cincotti F, Arendt-Nielsen L, Chen AC, Rossini PM. Anticipatory cortical responses during the expectancy of a predictable painful stimulation. A high-resolution electroencephalography study. *Eur J Neurosci*. 2003 Sep; 18(6): 1692–1700. [PubMed: 14511347]
- Berger H. Über das Elektrenkephalogramm des Menschen. *Archives für Psychiatrie*. 1929; 87:527–570.
- Biswal B, DeYoe AE, Hyde JS. Reduction of physiological fluctuations in fMRI using digital filters. *Magn Reson Med*. 1996 Jan; 35(1):107–113. [PubMed: 8771028]
- Bollimunta A, Mo J, Schroeder CE, Ding M. Neuronal mechanisms and attentional modulation of corticothalamic oscillations. *J Neurosci*. 2011 Mar 30; 31(13):4935–4943. [PubMed: 21451032]
- Brignani D, Manganotti P, Rossini PM, Miniussi C. Modulation of cortical oscillatory activity during transcranial magnetic stimulation. *Hum Brain Mapp*. 2008 May; 29(5):603–612. [PubMed: 17557296]
- Buckner RL, Andrews-Hanna JR, Schacter DL. The brain's default network: anatomy, function, and relevance to disease. *Ann N Y Acad Sci*. 2008 Mar. 1124:1–38. [PubMed: 18400922]
- Buckner RL, Sepulcre J, Talukdar T, Krienen FM, Liu H, Hedden T, Andrews-Hanna JR, Sperling RA, Johnson KA. Cortical hubs revealed by intrinsic functional connectivity: mapping, assessment of stability, and relation to Alzheimer's disease. *J Neurosci*. 2009 Feb 11; 29(6):1860–1873. [PubMed: 19211893]
- Candidi M, Stienen BM, Aglioti SM, de Gelder B. Event-related repetitive transcranial magnetic stimulation of posterior superior temporal sulcus improves the detection of threatening postural changes in human bodies. *J Neurosci*. 2011 Nov 30; 31(48):17547–17554. [PubMed: 22131416]
- Canolty RT, Soltani M, Dalal SS, Edwards E, Dronkers NF, Nagarajan SS, Kirsch HE, Barbaro NM, Knight RT. Spatiotemporal dynamics of word processing in the human brain. *Front Neurosci*. 2007 Nov; 1(1):185–196. Epub 2007 Oct 15. [PubMed: 18982128]
- Capotosto P, Babiloni C, Romani GL, Corbetta M. Frontoparietal cortex controls spatial attention through modulation of anticipatory alpha rhythms. *J Neurosci*. 2009; 29(18):5863–5872. [PubMed: 19420253]
- Capotosto P, Babiloni C, Romani GL, Corbetta M. Differential Contribution of Right and Left Parietal Cortex to the Control of Spatial Attention: A Simultaneous EEG-rTMS Study. *Cereb Cortex*. 2012a Feb; 22(2):446–454. [PubMed: 21666126]
- Capotosto P, Corbetta M, Romani GL, Babiloni C. Electrophysiological correlates of stimulus-driven reorienting deficits after interference with right parietal cortex during a spatial attention task: a TMS-EEG study. *J Cogn Neurosci*. 2012b Dec; 24(12):2363–2371. [PubMed: 22905824]
- Chadick JZ, Gazzaley A. Differential coupling of visual cortex with default or frontal-parietal network based on goals. *Nat Neurosci*. 2011 May 29; 14(7):830–832. [PubMed: 21623362]
- Corbetta M, Shulman GL. Control of goal-directed and stimulus-driven attention in the brain. *Nat Rev Neurosci*. 2002; 3:201–215. [PubMed: 11994752]
- Corbetta M, Shulman GL. Spatial neglect and attention networks. *Annu Rev Neurosci*. 2011; 34:569–599. Review. [PubMed: 21692662]
- Crone NE, Sinai A, Korzeniewska A. High-frequency gamma oscillations and human brain mapping with electrocorticography. *Prog Brain Res*. 2006; 159:275–295. Review. [PubMed: 17071238]
- Dastjerdi M, Foster BL, Nasrullah S, Rauschecker AM, Dougherty RF, Townsend JD, Chang C, Greicius MD, Menon V, Kennedy DP, Parvizi J. Differential electrophysiological response during

- rest, self-referential, and non-self-referential tasks in human posteromedial cortex. *Proc Natl Acad Sci U S A*. 2011 Feb 15; 108(7):3023–3028. Epub 2011 Jan 31. [PubMed: 21282630]
- Deco G, Corbetta M. The dynamical balance of the brain at rest. *Neuroscientist*. 2011 Feb; 17(1):107–123. Epub 2010 Dec 31. [PubMed: 21196530]
- de Pasquale F, Della Penna S, Snyder AZ, Marzetti L, Pizzella V, Romani GL, Corbetta M. A cortical core for dynamic integration of functional networks in the resting human brain. *Neuron*. 2012 May 24; 74(4):753–764. [PubMed: 22632732]
- Fox MD, Raichle ME. Spontaneous fluctuations in brain activity observed with functional magnetic resonance imaging. *Nat Rev Neurosci*. 2007 Sep; 8(9):700–711. Review. [PubMed: 17704812]
- Fox MD, Snyder AZ, Vincent JL, Corbetta M, Van Essen DC, Raichle ME. The human brain is intrinsically organized into dynamic, anticorrelated functional networks. *Proc Natl Acad Sci U S A*. 2005 Jul 5; 102(27):9673–9678. [PubMed: 15976020]
- Freunberger R, Klimesch W, Sauseng P, Griesmayr B, Höller Y, Pecherstorfer T, Hanslmayr S. Gamma oscillatory activity in a visual discrimination task. *Brain Res Bull*. 2007 Mar 30; 71(6):593–600. Epub 2006 Dec 27. [PubMed: 17292802]
- Friese U, Supp GG, Hipp JF, Engel AK, Gruber T. Oscillatory MEG gamma band activity dissociates perceptual and conceptual aspects of visual object processing: a combined repetition/conceptual priming study. *Neuroimage*. 2012 Jan 2; 59(1):861–871. Epub 2011 Jul 30. [PubMed: 21835246]
- Fries P. A mechanism for cognitive dynamics: neuronal communication through neuronal coherence. *Trends Cogn Sci*. 2005 Oct; 9(10):474–480. Review. [PubMed: 16150631]
- Funke K, Benali A. Cortical cellular actions of transcranial magnetic stimulation. *Restor Neurol Neurosci*. 2010; 28(4):399–417. Review. [PubMed: 20714065]
- Gonçalves SI, de Munck JC, Pouwels PJ, Schoonhoven R, Kuijter JP, Maurits NM, Hoogduin JM, Van Someren EJ, Heethaar RM, Lopes da Silva FH. Correlating the alpha rhythm to BOLD using simultaneous EEG/fMRI: inter-subject variability. *Neuroimage*. 2006 Mar; 30(1):203–213. [PubMed: 16290018]
- Hagmann P, Cammoun L, Gigandet X, Meuli R, Honey CJ, Wedeen VJ, Sporns O. Mapping the structural core of human cerebral cortex. *PLoS Biol*. 2008 Jul 1.6(7):e159. [PubMed: 18597554]
- Haegens S, Luther L, Jensen O. Somatosensory anticipatory alpha activity increases to suppress distracting input. *J Cogn Neurosci*. 2012 Mar; 24(3):677–685. [PubMed: 22066587]
- Harris IM, Benito CT, Ruzzoli M, Miniussi C. Effects of right parietal transcranial magnetic stimulation on object identification and orientation judgments. *J Cogn Neurosci*. 2008; 20(5):916–926. [PubMed: 18201128]
- He BJ, Snyder AZ, Vincent JL, Epstein A, Shulman GL, Corbetta M. Breakdown of functional connectivity in frontoparietal networks underlies behavioral deficits in spatial neglect. *Neuron*. 2007; 53(6):905–918. [PubMed: 17359924]
- Klimesch W, Doppelmayr M, Russegger H, Pachinger T, Schwaiger J. Induced alpha band power changes in the human EEG and attention. *Neurosci Lett*. 1998; 244:73–76. [PubMed: 9572588]
- Knyazev GG, Slobodskoj-Plusnin JY, Bocharov AV, Pyrkova LV. The default mode network and EEG  $\alpha$  oscillations: an independent component analysis. *Brain Res*. 2011 Jul 21.1402:67–79. Epub 2011 May 27. [PubMed: 21683942]
- Laufs K, Krakow P, Sterzer E, Eger A, Beyerle A, Salek-Haddadi A, Kleinschmidt A. Electroencephalographic signatures of attentional and cognitive default modes in spontaneous brain activity at rest *Proc. Natl. Acad. Sci. U.S.A.* 2003; 100:11053–11058.
- Lewis CM, Baldassarre A, Committeri G, Romani GL, Corbetta M. Learning sculpts the spontaneous activity of the resting human brain. *Proc Natl Acad Sci U S A*. 2009 Oct 13; 106(41):17558–17563. [PubMed: 19805061]
- Liu H, Stufflebeam SM, Sepulcre J, Hedden T, Buckner RL. Evidence from intrinsic activity that asymmetry of the human brain is controlled by multiple factors. *Proc Natl Acad Sci U S A*. 2009 Dec 1; 106(48):20499–20503. [PubMed: 19918055]
- Lorincz ML, Kékesi KA, Juhász G, Crunelli V, Hughes SW. Temporal framing of thalamic relay-mode firing by phasic inhibition during the alpha rhythm. *Neuron*. 2009 Sep 10; 63(5):683–696. [PubMed: 19755110]

- Machii K, Cohen D, Ramos-Estebanez C, Pascual-Leone A. Safety of rTMS to non-motor cortical areas in healthy participants and patients. *Clin Neurophysiol.* 2006; 117:455–471. [PubMed: 16387549]
- Mantini D, Perrucci MG, Del Gratta C, Romani GL, Corbetta M. Electrophysiological signatures of resting state networks in the human brain. *Proc Natl Acad Sci U S A.* 2007; 104(32):13170–13175. [PubMed: 17670949]
- Miller KJ, Weaver KE, Ojemann JG. Direct electrophysiological measurement of human default network areas. *Proc Natl Acad Sci USA.* 2009; 106:12174–12177. [PubMed: 19584247]
- Mutanen T, Mäki H, Ilmoniemi RJ. The effect of stimulus parameters on TMS-EEG muscle artifacts. *Brain Stimul.* 2013 May; 6(3):371–376. [PubMed: 22902312]
- Pfurtscheller G, Lopes da Silva FH. Event-related EEG/MEG synchronization and de-synchronization: basic principles. *Clin Neurophysiol.* 1999; 110:1842–1857. [PubMed: 10576479]
- Pfurtscheller G, Andrew C. Event-related changes of band power and coherence: methodology and interpretation. *J Clin Neurophysiol.* 1999; 16(6):512–519. (1999). [PubMed: 10600019]
- Raichle ME, MacLeod AM, Snyder AZ, Powers WJ, Gusnard DA, Shulman GL. A default mode of brain function. *Proc Natl Acad Sci U S A.* 2001 Jan 16; 98(2):676–682. [PubMed: 11209064]
- Rappelsberger P, Petsche H. Probability mapping: power and coherence analyses of cognitive processes. *Brain Topogr.* 1988; 1(1):46–54. (1988). [PubMed: 3274962]
- Ridding MC, Ziemann U. Determinants of the induction of cortical plasticity by non-invasive brain stimulation in healthy subjects. *J Physiol.* 2010 Jul 1; 588(Pt 13):2291–2304. Epub 2010 May 17. [PubMed: 20478978]
- Rossi S, Hallett M, Rossini PM, Pascual-Leone A. Safety of TMS Consensus Group. Safety, ethical considerations, and application guidelines for the use of transcranial magnetic stimulation in clinical practice and research. *Clin Neurophysiol.* 2009; 120(12):2008–2039. [PubMed: 19833552]
- Rossini PM, Barker AT, Berardelli A, Caramia MD, Caruso G, Cracco RQ, Dimitrijević MR, Hallett M, Katayama Y, Lücking CH. Non invasive electrical and magnetic stimulation of the brain, spinal cord and roots: Basic principles and procedures for routine clinical application. *Electroencephalography and Clinical Neurophysiology.* 1994; 91:79–92. [PubMed: 7519144]
- Sadaghiani S, Scheeringa R, Lehongre K, Morillon B, Giraud AL, Kleinschmidt A. Intrinsic connectivity networks, alpha oscillations, and tonic alertness: a simultaneous electroencephalography/functional magnetic resonance imaging study. *J Neurosci.* 2010 Jul 28; 30(30):10243–10250. [PubMed: 20668207]
- Sestieri C, Shulman GL, Corbetta M. Attention to memory and the environment: functional specialization and dynamic competition in human posterior parietal cortex. *J Neurosci.* 2010 Jun 23; 30(25):8445–8456. [PubMed: 20573892]
- Sestieri C, Corbetta M, Romani GL, Shulman GL. Episodic memory retrieval, parietal cortex, and the default mode network: functional and topographic analyses. *J Neurosci.* 2011 Mar 23; 31(12):4407–4420. [PubMed: 21430142]
- Sestieri C, Capotosto P, Tosoni A, Luca Romani G, Corbetta M. Interference with episodic memory retrieval following transcranial stimulation of the inferior but not the superior parietal lobule. *Neuropsychologia.* 2013 Feb 4; 51(5):900–906. [PubMed: 23391557]
- Siegel M, Donner TH, Oostenveld R, Fries P, Engel AK. Neuronal synchronization along the dorsal visual pathway reflects the focus of spatial attention. *Neuron.* 2008 Nov 26; 60(4):709–719. [PubMed: 19038226]
- Shulman GL, Ongür D, Akbudak E, Conturo TE, Ollinger JM, Snyder AZ, Gusnard DA, Raichle ME. Common blood flow changes across visual tasks: II. Decreases in cerebral cortex. *J Cogn Neurosci.* 1997; 9:648–663. [PubMed: 23965122]
- Shulman GL, Pope DL, Astafiev SV, McAvoy MP, Snyder AZ, Corbetta M. Right hemisphere dominance during spatial selective attention and target detection occurs outside the dorsal frontoparietal network. *J Neurosci.* 2010 Mar 10; 30(10):3640–3651. [PubMed: 20219998]
- Smith SM, Fox PT, Miller KL, Glahn DC, Fox PM, Mackay CE, Filippini N, Watkins KE, Toro R, Laird AR, Beckmann CF. Correspondence of the brain's functional architecture during activation and rest. *Proc Natl Acad Sci U S A.* 2009 Aug 4; 106(31):13040–13045. Epub 2009 Jul 20. [PubMed: 19620724]

- Srinivasan R, Winter WR, Nunez PL. Prog Brain Res. 2006; 159:29–42. [PubMed: 17071222]
- Steriade M, Datta S, Paré D, Oakson G, Curró Dossi RC. Neuronal activities in brain-stem cholinergic nuclei related to tonic activation processes in thalamocortical systems. J Neurosci. 1990 Aug; 10(8):2541–2559. [PubMed: 2388079]
- Thickbroom GW. Transcranial magnetic stimulation and synaptic plasticity: experimental framework and human models. Exp Brain Res. 2007 Jul; 180(4):583–593. Epub 2007 Jun 12. Review. [PubMed: 17562028]
- Thut G, Nietzel A, Brandt SA, Pascual-Leone A. Alpha-band electroencephalographic activity over occipital cortex indexes visuospatial attention bias and predicts visual target detection. J Neurosci. 2006; 26:9494–9502. [PubMed: 16971533]
- Trippe J, Mix A, Aydin-Abidin S, Funke K, Benali A. è burst and conventional low-frequency rTMS differentially affect GABAergic neurotransmission in the rat cortex. Exp Brain Res. 2009 Dec; 199(3–4):411–421. [PubMed: 19701632]
- Urgesi C, Calvo-Merino B, Haggard P, Aglioti SM. Transcranial magnetic stimulation reveals two cortical pathways for visual body processing. J Neurosci. 2007 Jul 25; 27(30):8023–8030. [PubMed: 17652592]
- Urgesi C, Berlucchi G, Aglioti SM. Magnetic stimulation of extrastriate body area impairs visual processing of nonfacial body parts. Curr Biol. 2004 Dec 14; 14(23):2130–2134. [PubMed: 15589156]
- Vaishnavi SN, Vlassenko AG, Rundle MM, Snyder AZ, Mintun MA, Raichle ME. Regional aerobic glycolysis in the human brain. Proc Natl Acad Sci U S A. 2010 Oct 12; 107(41):17757–17762. [PubMed: 20837536]
- Wassermann EM. Risk and safety of repetitive transcranial magnetic stimulation: report and suggested guidelines from the International Workshop on the Safety of Repetitive Transcranial Magnetic Stimulation, June 5–7, 1996. Electroencephalogr Clin Neurophysiol. 1998; 108:1–16. [PubMed: 9474057]
- Worden MS, Foxe JJ, Wang N, Simpson GV. Anticipatory biasing of visuospatial attention indexed by retinotopically specific alpha-band electroencephalography increases over occipital cortex. J Neurosci. 2000; 20:RC63. [PubMed: 10704517]
- Wu L, Eichele T, Calhoun VD. Reactivity of hemodynamic responses and functional connectivity to different states of alpha synchrony: a concurrent EEG-fMRI study. Neuroimage. 2010 Oct 1; 52(4):1252–1260. [PubMed: 20510374]

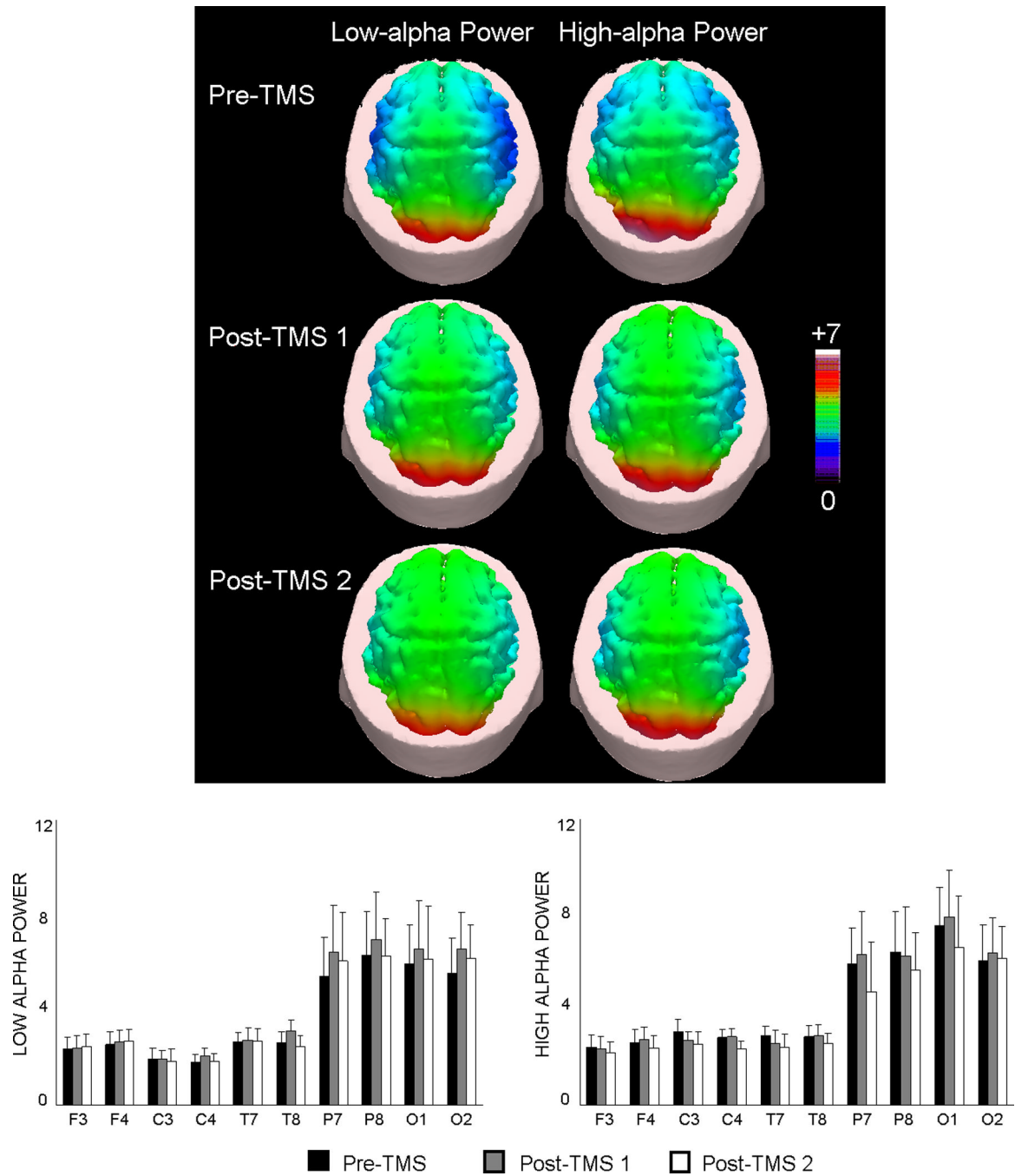


**Figure 1. Topography of low- and high- frequency alpha power density in the Sham condition: top**

Topographic maps of low- and high-frequency alpha power density during the three periods of interest (Pre-TMS, Post-TMS 1, Post-TMS 2). Bottom: Group means ( $\pm$  SE) of the low- and high-frequency alpha power density in the Sham condition.



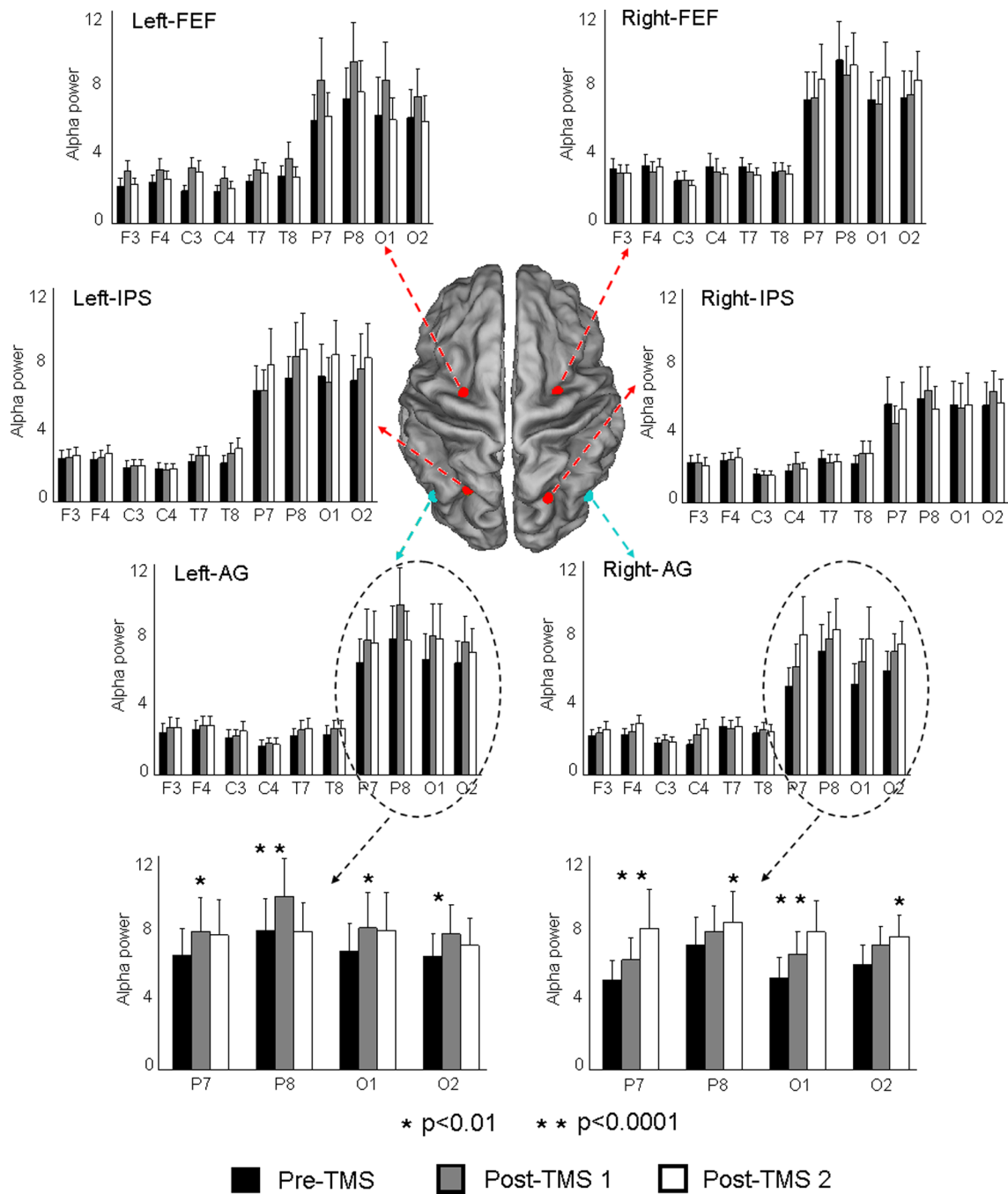


**Figure 2. Alpha power density**

Group means ( $\pm$  SE) of the low-frequency alpha power density for all active magnetic stimulation sites (i.e., Right-AG, Left-AG, Right-IPS, Left-IPS, Right-FEF, Left-FEF) and periods of interest (pre-TMS, post-TMS 1, post-TMS 2). Duncan post-hoc test: statistically significant differences between pre- and post-TMS periods are indicated by one ( $p < 0.01$ ) or two ( $p < 0.0001$ ) asterisks.

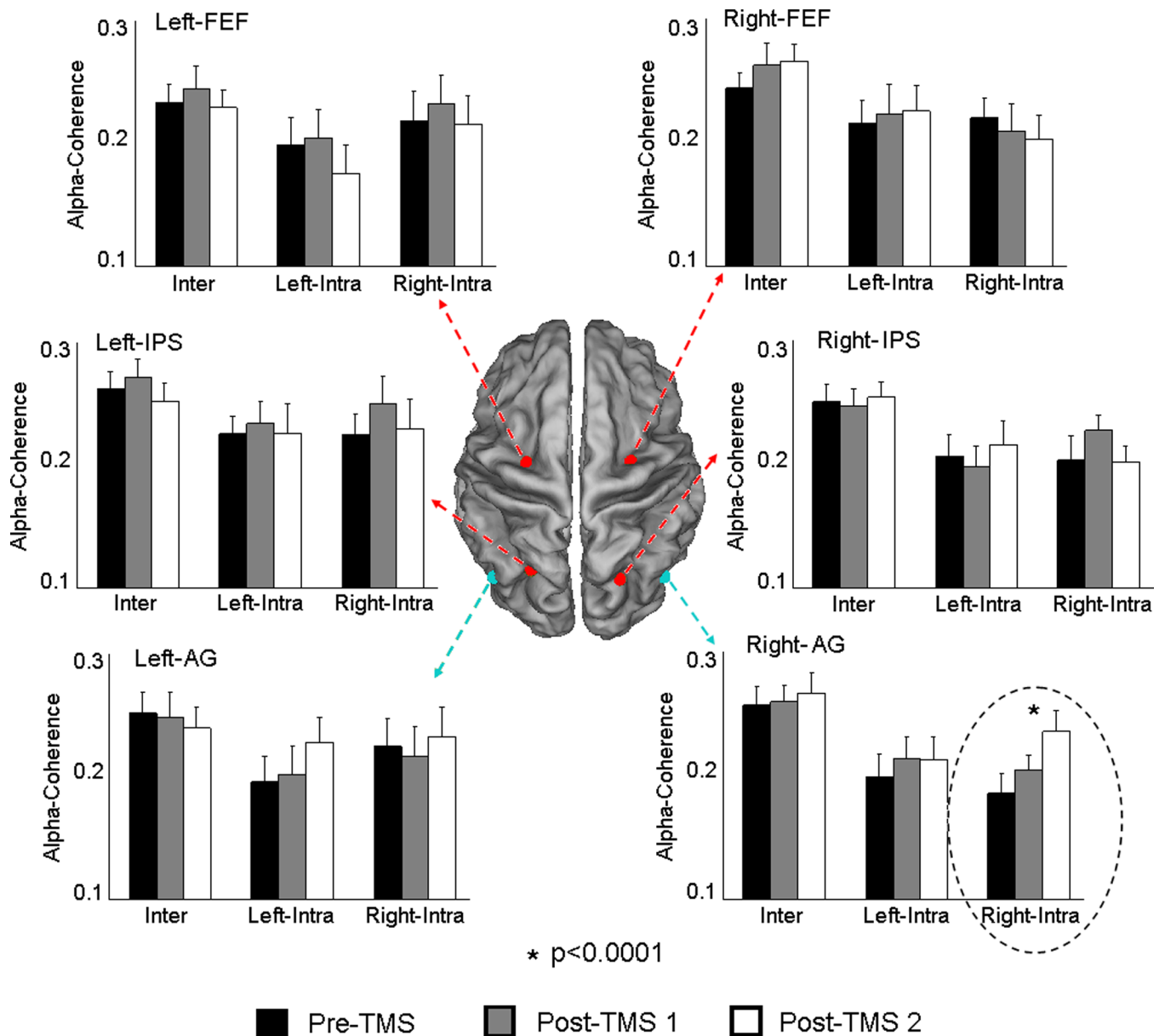


**Figure 3. Alpha coherence**

Group means ( $\pm$  SE) of the low-frequency alpha inter- and intra hemispheric coherence for all active magnetic stimulation sites (i.e., Right-AG, Left-AG, Right-IPS, Left-IPS, Right-FEF, Left-FEF) and periods of interest (pre-TMS, post-TMS 1, post-TMS 2). Duncan post-hoc test: statistically significant differences between pre- and post-TMS periods are indicated by one asterisk ( $p < 0.0001$ ).

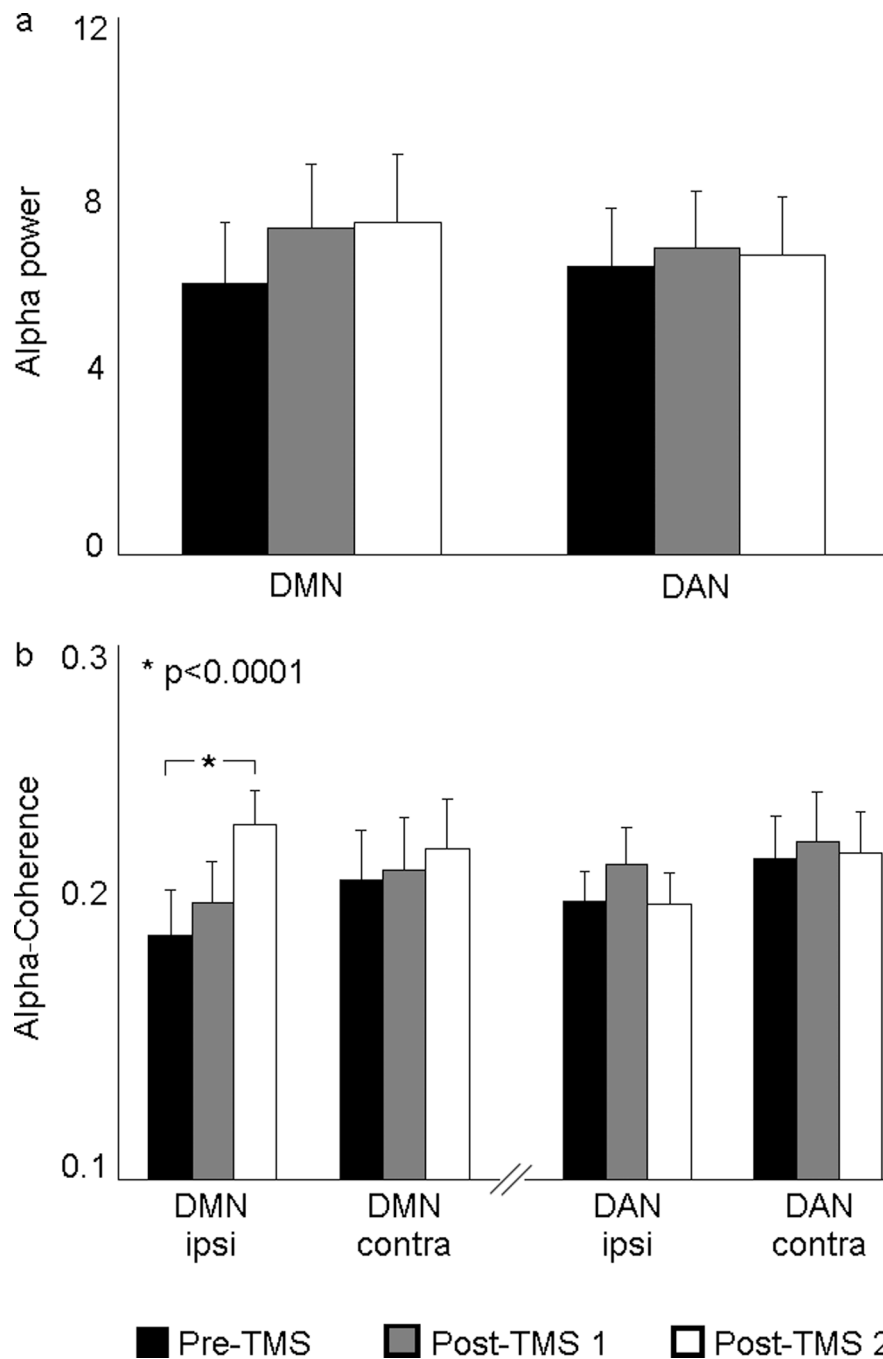


**Figure 4. DMN vs DAN**

a) Group means ( $\pm$  SE) of the low-frequency alpha power density for the two Networks (DMN and DAN) and periods of interest (pre-TMS, post-TMS 1, post-TMS 2). b) Group means ( $\pm$  SE) of the low-frequency alpha intra hemispheric coherence for the two Networks (DMN and DAN) and periods of interest (pre-TMS, post-TMS 1, post-TMS 2), separated by Hemisphere (ipsilateral and contralateral to the stimulation). Duncan post-hoc test: statistically significant differences between pre- and post-TMS periods are indicated by one asterisk ( $p < 0.0001$ ).

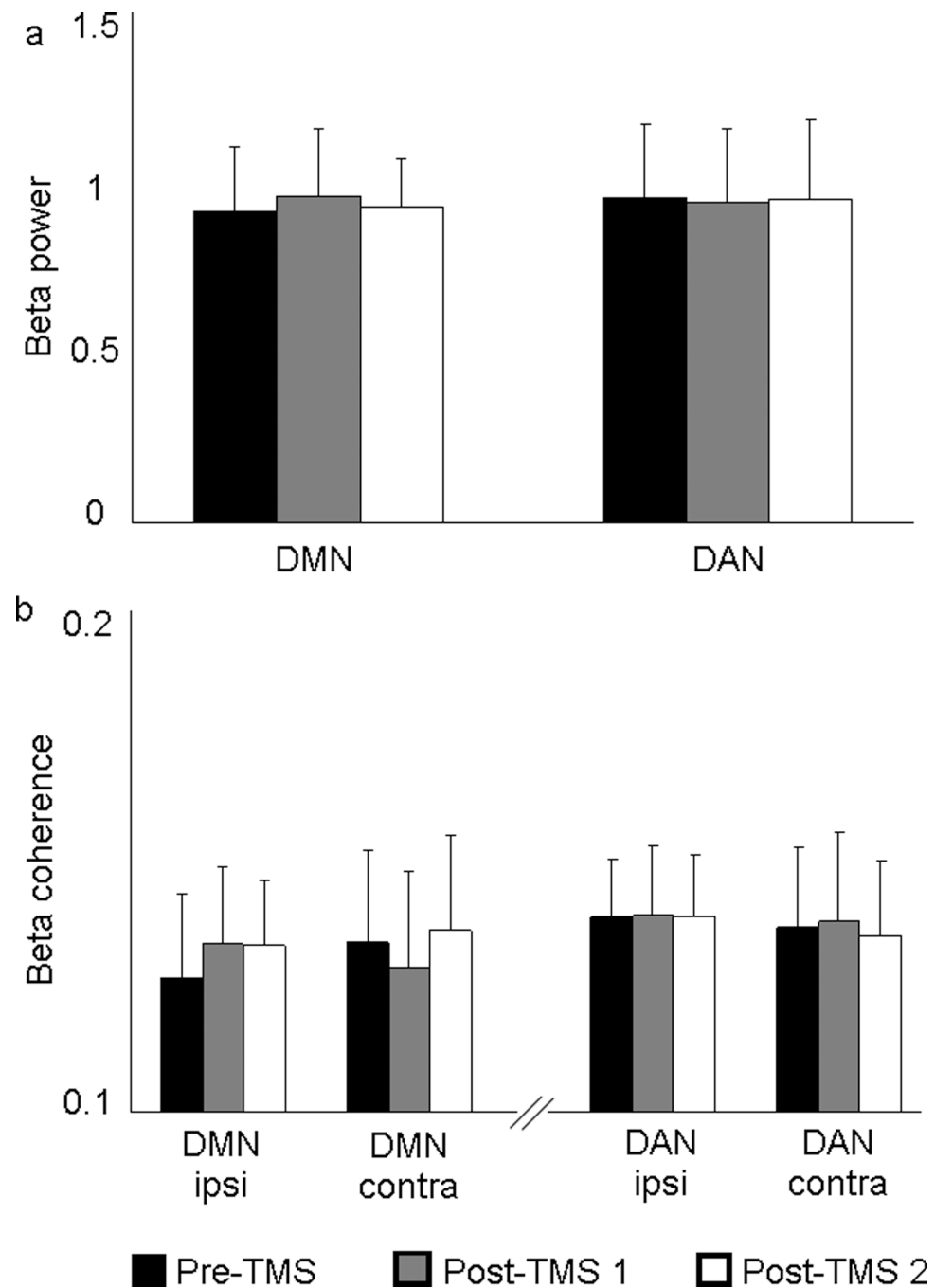


**Figure 5. DMN vs DAN in the beta band**

a) Group means ( $\pm$  SE) of the beta power density for the two Networks (DMN and DAN) and periods of interest (pre-TMS, post-TMS 1, post-TMS 2). b) Group means ( $\pm$  SE) of the beta intra hemispheric coherence for the two Networks (DMN and DAN) and periods of interest (pre-TMS, post-TMS 1, post-TMS 2), separated by Hemisphere (ipsilateral and contralateral to the stimulation).